ISSN 1330-3651 (Print), ISSN 1848-6339 (Online) https://doi.org/10.17559/TV-20240217001329
Original scientific paper

Efficient Net-Based Deep Learning for Visual Fault Detection in Solar Photovoltaic Modules

R. PRIYADARSHINI*, P. S. MANOHARAN, S. MOHAMED MANSOOR ROOMI

Abstract: Detecting faults in solar photovoltaic modules (PVM) is crucial for enhancing their longevity, power output, and overall reliability. Visual anomalies such as soiling, partial shading, cell damage, and glass breakage pose significant challenges for fault identification, particularly in harsh environmental conditions. Therefore, it is essential to maintain healthy PV systems with extended lifecycles and optimal performance through the quick and efficient detection of faults. This work introduces a comprehensive approach that encompasses dataset creation, preprocessing, and PV fault classification utilizing the EfficientNet B0 model. Processed RGB images serve as input for the model, enabling the classification of visual faults in PVM. The performance evaluation of the proposed deep neural network model includes metrics such as classification accuracy, *F*1 score, specificity, and recall. The results highlight the exceptional performance of the proposed model, achieving a classification accuracy of 97.24% for visual fault identification in PV modules. Moreover, the study underscores the model's robustness and efficacy through a comparative analysis with other classification techniques reported in the literature.

Keywords: deep neural network; RGB images; solar photovoltaic modules; visual anomalies

1 INTRODUCTION

Global energy demand is rising at an annual rate of 2,1%, which is twice the rate of energy supply growth, predominantly driven by fossil fuels (79,7%) [1]. This reliance on fossil fuels is contributing significantly to greenhouse gas emissions, climate change, and global warming [2]. With the reserves of coal, oil, and gas depleting, the shift to renewable energy sources has become essential. Among these, solar and wind energy are particularly critical, with solar power being available throughout the year. Photovoltaic Modules (PVM) are fundamental for converting solar irradiance into electricity; however, the maintenance of solar farms presents challenges, such as land use, high costs, and the need for timely fault detection. Traditional manual assessments, conducted every three months, are both resource-intensive and prone to errors. Electrical faults in PVMs, such as line-to-line and line-to-ground conditions, can be detected using system parameters like DC voltage, DC current, insolation, output power, power-voltage curves, and current-voltage curves. Various feature extraction techniques, such as Fourier transforms [3], wavelet transforms [4], and statistical measures [5], are employed to extract relevant features, which are then input into machine learning models [6] like Artificial Neural Networks (ANN) [7], decision trees, K-Nearest Neighbors (kNN) [8], Support Vector Machines (SVM) [9], and Deep Belief Networks (DBN). These methods enhance the accuracy and efficiency of data analysis. Environmental factors, such as temperature and climatic conditions, can also serve as features for fault detection and classification [10]. Unmanned Aerial Vehicles (UAVs) are increasingly being used to inspect PVMs [11], offering efficiency, reduced energy usage, and less dependence on human intervention. Equipped with high-resolution digital cameras, UAVs capture true-color images that are processed using various techniques to identify subtle faults, such as snail tracks, glass breakage, and delamination. These processes involve machine learning and deep learning, covering image pre-processing, salient feature extraction, and classification. Image preprocessing techniques include histogram equalization, noise removal, and resizing. Salient features, extracted using methods such as moving averages and Histogram of Oriented Gradients (HOG), are used to train algorithms like kNN, Naive Bayes, and Random Forest. Notably, the Naive Bayesian classifier achieved an accuracy of 94.1% when applied to three thermal image fault classes: Defective, Non-defective with hotspots (NDH), and Non-defective without hotspots (NDNH) [12]. Sridharan et al. compared various transfer learning models, including VGG16, GoogLeNet, and ResNet50, in addition to ML algorithms such as Naive Bayes, SVM, kNN, Decision Tree, and Random Tree for feature extraction and fault classification [13]. In the field of solar cell research, Electroluminescent PV cells are gaining attention for their potential to improve solar panel efficiency and durability. A recent study demonstrated the use of a combination of Convolutional Neural Networks (CNN) and Random Forest algorithms to detect Electroluminescent PV cells with remarkable accuracy, achieving a 95.07% success rate [14]. This approach holds great potential for improving the reliability of solar panels and advancing solar energy research. Random Forest models have also been successful in addressing PVM errors, enhancing diagnostic efficiency for numerical data. Furthermore, a recent study introduced automatic fault detection in photovoltaic cells using RGB [13], thermal [15], and infrared (IR) imaging. Germán et al. proposed a two-stage inspection method for PV plants using infrared thermography, combining aerial and ground-level inspections for a comprehensive analysis. This method improves fault detection and facilitates timely resolution of issues in PV plants [16]. Deep learning models also utilize image processing techniques such as texture analysis and descriptors to enhance fault detection and classification in solar PV systems. A failure mode recognition algorithm, based on deep learning, has been developed to classify faults such as sealant discoloration, glass cracks, sealant delamination, and powder tarnish. VGG16 deep features are extracted and classified using SVM for PVM fault classification [16]. Moreover, a Cascading AutoEncoder (CASAE), an advanced machine

learning technique, has achieved an accuracy of 93.02% in detecting flaws on metal surfaces, including dust occurrence, damage spots, and glue marks. CASAE's precision makes it a valuable tool for maintaining metal surfaces by facilitating early detection and quick, cost-effective repairs [17]. Akram et al. applied CNN to detect faults in electroluminescence images with an accuracy of 93.02%, demonstrating the potential of CNN for efficient fault detection [18]. Li et al. used deep learning to diagnose faults in large-scale PV farms, employing a CNN-based feature extraction and classification model with seven layers [19]. Duranay et al. explored the classification of defects in PVMs using IR images and employed the EfficientNet B0 model to extract 17000 features, achieving a 93,93% average accuracy with the SVM classifier [20]. Cavieres et al. used Region-Based Convolutional Neural Networks (RCNN) to detect and identify modules in PV systems, predicting their performance with 73% accuracy through supervised learning algorithms [21]. Existing literature emphasizes the impact of solar PV conditions - such as cell damage, breakage, soiling, partial shading, and normal operation-on panel efficiency, yet there is limited coverage. Visual faults, including shading, dirt accumulation, surface cracks, damage, and corrosion, significantly reduce energy production. While many deep learning approaches exist for fault recognition in solar PVMs using electroluminescence, thermal, and IR imaging, there remains a need for methods utilizing conventional RGB photography. The challenge lies in the availability of larger RGB datasets, which are crucial for deep learning models. To address this gap, this work proposes the use of the EfficientNet B0 model on an RGB dataset containing 11250 images to improve fault recognition and classification in solar PV systems. The key contributions of this study are as follows:

- Development and compilation of a Photovoltaic Fault Image Dataset, featuring cases such as Normal, Breakage, Cell Damage, Partial Shading, and Soiling.
- Implementation of a robust fault detection approach using the EfficientNet B0 model.
- Empirical validation of the fault classification model using pre-trained models and state-of-the-art techniques.

Section 2 discusses solar PV fault image data collection, Section 3 outlines the proposed methodology for PV fault classification, Section 4 presents the outcomes and discussion, and Section 5 concludes the study.

2 DATABASE COLLECTION

To address the issue of limited data availability, the authors compiled a comprehensive RGB image dataset for PV faults, including partial shading, breakage, soiling, and cell damage. This dataset was created by aggregating images from both online sources and real-time captures. Tab. 1 provides an overview of the local RGB dataset, which was captured under various conditions using 12 MP and 5 MP camera systems. Images were taken at resolutions of 3024 × 4032 (26 mm) and 1920 × 1080 (25 mm), across different environmental conditions and angles (0°, 25°, 45°, 90°). These shooting angles were strategically selected to optimize fault detection.

Table 1 Details of the local dataset

Dataset Name	Types of PV faults	Images from Online source	Images captured locally	Number of images augmentation	
				Before	After
Local RGB dataset	Normal	83	115	198	2250
	Breakage	78	110	188	2250
	Cell Damage	83	55	138	2250
	Partial Shading	75	117	192	2250
	Soiling	117	78	195	2250

Initially, the collected images were screened to isolate RGB formats, as the transfer learning model exclusively processes this type. Fig. 1 highlights the imbalanced sample distribution across the different classes. To address this imbalance and expand the dataset, various augmentation techniques were applied, including 90 degree rotation, 0,5 scaling along the x and y axes, 45 degree shearing along the x and y axes, and translation, either individually or in combination. These augmentation methods increased the dataset from 911 to 11250 images, with each class containing 2250 images.

3 PROPOSED METHODOLOGY

This research proposes an artificial intelligence model for classifying PV faults, including partial shading, breakage, soiling, and cell damage. This section outlines the proposed methodology, covering database creation, image preprocessing, and solar PV fault classification using EfficientNet B0 transfer learning. Drone cameras are used to capture images at the solar plant, with the intelligent system classifying PV module conditions through transfer learning (Fig. 2). The image preprocessing stage involves removing irrelevant images, resizing, and augmentation. All images are standardized to dimensions of 224 × 224 × 3. In this study, 80% of the augmented data is used to train the classification model, while the remaining 20% is used for testing. EfficientNet B0 is employed for PV fault classification during training. Transfer learning is a highly effective deep learning technique that leverages pre-trained models to accelerate training, improve accuracy, and reduce the need for large datasets. This is particularly useful in scenarios with limited data or high computational costs. One such pre-trained model is EfficientNet-B0, a convolutional neural network (CNN) trained on the large-scale ImageNet dataset, making it highly proficient in image classification tasks. With 5.3 million parameters, it optimizes performance and efficiency through depth, width, and resolution scaling. EfficientNet-B0 has achieved state-of-the-art results, with an impressive 84,4% accuracy on ImageNet, surpassing previous models while using fewer parameters and computational resources (Fig. 3).

The weighted scale comprising of the model hyperparameters such as stated in Eq. (1), namely depth d, width w, and resolution r defined as:

$$\text{Depth: } d = A^{\varphi}, \text{ width: } w = B^{\varphi}.$$

$$\text{Resolution: } d = \Gamma^{\varphi} \tag{1}$$

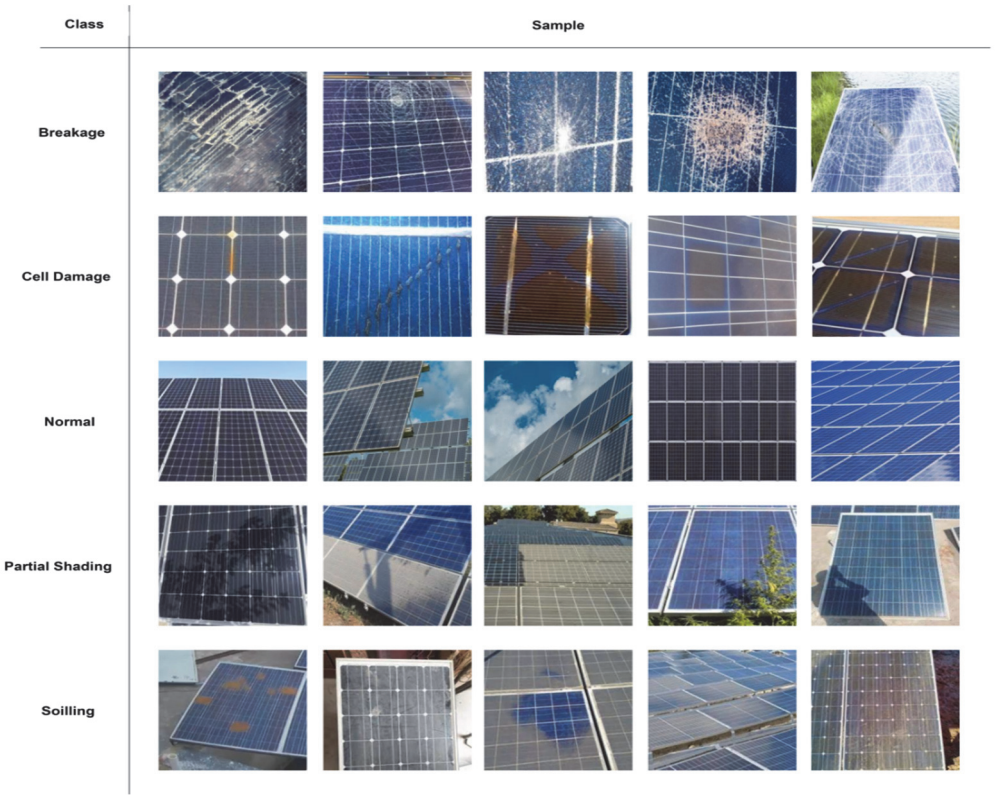

Figure 1 Sample Images from the dataset collected

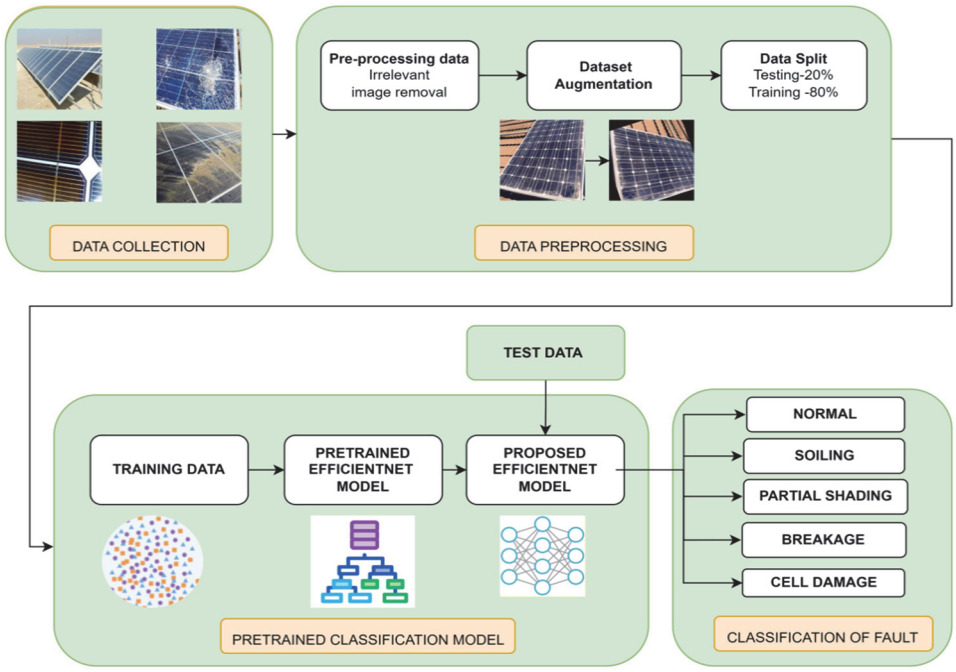

Figure 2 Proposed method for fault classification

Initially, the constants A, B, and Γ are defined, which determine the network's resolution. The compound coefficient Ø is initially set to 1, defining the base configuration, EfficientNetB0. The architecture of EfficientNet-B0 consists of three main modules: the Head, the Stem, and the Blocks. The Stem includes a convolutional layer with a kernel size of (3 × 3), a batch normalization (BN) layer, and a Swish activation function. The core of the architecture lies in the Blocks, which consist of multiple Mobile Inverted Bottleneck Convolutions (MBConv). EfficientNet-B0 employs MBConv1 and MBConv6, where the numbers 1 and 6 represent the expansion ratios. MBConv1 includes a Depthwise Convolution (DwC), followed by BN, Swish, Squeeze-and-Excitation (SE), Convolution, and BN layers, repeated three times. MBConv6 consists of a Convolution layer, a DwC layer between two pairs of BN and Swish activations, and additional BN layers repeated four times, similar to MBConv1. The SE block enhances inter-channel dependencies by dynamically recalibrating feature channels for optimal weighting. The Head module comprises a Convolution layer, BN, Swish, Pooling, Dropout, and Fully Connected layers. Tab. 2 outlines the

structure of the pre-trained model, which features 9 stages and 237 layers.

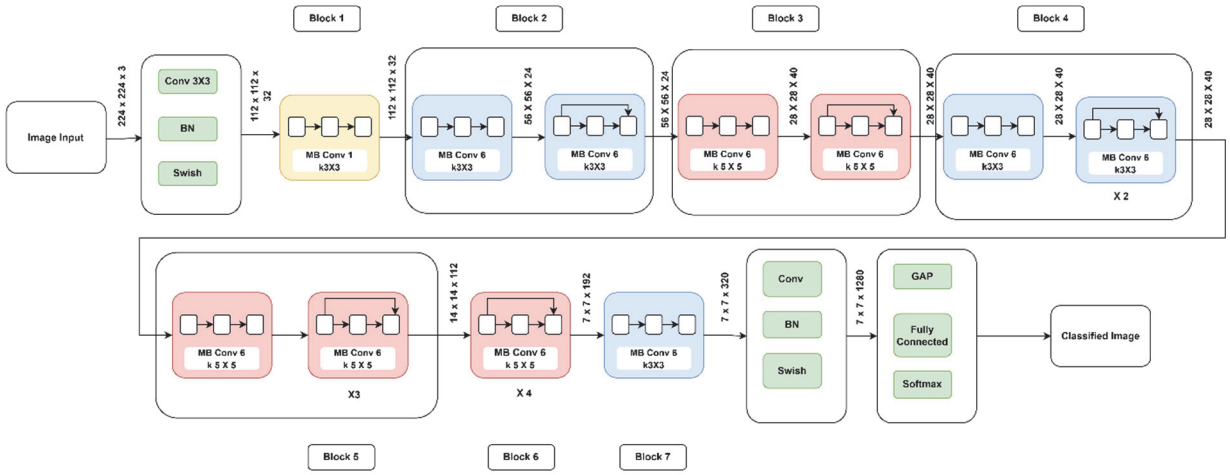

Figure 3 Layer architecture of Efficientnet B0 for PV fault classification

Table 2 Layer description of efficient net B0

Stage	Operator	Resolution	#Channels	#Layers
1	Conv 3 × 3	224 × 224	32	1
2	MBConv1, *k*3 × 3	112 × 112	16	1
3	MBConv6, *k*3 × 3	112 × 112	24	2
4	MBConv6, *k*5 × 5	56 × 56	40	2
5	MBConv6, *k*3 × 3	28 × 28	80	3
6	MBConv6, *k*5 × 5	14 × 14	112	3
7	MBConv6, *k*5 × 5	14 × 14	192	4
8	MBConv6, *k*3 × 3	7 × 7	320	1
9	Conv 1 × 1 & Pooling & FC	7 × 7	1280	1

EfficientNet B0 employs Global Average Pooling layers and dropout layers, which are advantageous for avoiding overfitting. The Global Average Pooling layer has zero parameters to optimize, while the dropout layer prevents co-adaptation among neurons. When using a Global Average Pooling layer, the feature map is transformed into a feature set of size (1, *N*3), where *N*3 represents the number of filters used, and (*N*1, *N*2) corresponds to the image dimensions. A dropout layer in a neuron can be mathematically modelled as follows:

$$f(\kappa,\rho)=\begin{cases}\kappa, & \kappa=1\\ 1-\rho, & \kappa=0\end{cases} \tag{2}$$

where:
κ signifies the fault class
ρ is the probability of the real-valued representations, showing activated ($\rho = 0$) or deactivated ($\rho = 1$) neuron.

3.1 Performance Metrics

The effectiveness of the method for detecting faults in PV has been evaluated using the metrics of Precision, Recall, F1 Score, Micro Average Precision, and Macro Average Precision, as represented in Eq. (3), Eq. (4), Eq. (5), Eq. (6), and Eq. (7).

$$Precision(P)=\frac{TP}{(TP+FP)} \tag{3}$$

$$Recall(R)=\frac{TP}{(TP+FN)} \tag{4}$$

$$F1\ Score=\frac{2\cdot(Precision\cdot Recall)}{Precision+Recall} \tag{5}$$

$$\text{Micro Average Precision} = \frac{T_{p1}+T_{p2}\ \ldots\ T_{PN}}{\left(\left(T_{p1}+T_{p2}\ \ldots\ T_{PN}\right)+\left(F_{p1}+F_{p2}\ \ldots\ F_{PN}\right)\right)} \tag{6}$$

$$\text{Macro Average Precision} = \frac{P_1+P_2\ \ldots\ P_N}{N} \tag{7}$$

4 RESULTS AND DISCUSSION

This study assesses the efficiency of the EfficientNet-B0 transfer learning model using a local RGB dataset of 11,250 images for analyzing faults in solar PV modules. The model was trained on an HP server with 8 GB RAM, using Matlab 2022b, and pre-processed 224 × 224 × 3 images, with hyperparameters outlined in Tab. 3. Hyperparameter tuning had a significant impact on performance, with training accuracy ranging from 85% to 92%. Stochastic Gradient Descent with Momentum (SGDM) achieved 97,2% accuracy by epoch 10 but fluctuated notably with changes in epochs and learning rates, dropping to 95,5%. The model's performance improved considerably with smaller learning rates and a greater number of epochs, with the optimized parameters detailed in Tab. 4. Grad-CAM [15] is a visual explanation technique that can be applied to any CNN-based network without requiring changes to the architecture. It uncovers attention focus discrepancies, enabling effective differentiation of fault classes. The importance map is generated by computing the derivative of the output of the reduction layer with respect to a convolutional feature map for each class. The Grad-CAM visualizations for the EfficientNet-B0 model, as well as other models such as SqueezeNet, ResNet-18, GoogLeNet, and MobileNet, are

shown in Fig. 4. These images demonstrate that the EfficientNet-B0 model primarily focuses on faults occurring in solar PV modules, as indicated by the Grad-CAM heat map. It highlights the regions of fault occurrence while de-emphasizing other areas of the solar PV panel. This leads to more accurate fault localization, with a precise emphasis on the faulty regions. The training plot for the EfficientNet-B0 model shows a classification training accuracy of 97,52% after tuning (Fig. 5). The minimal disparity between training and testing accuracies indicates robust learning. However, some testing accuracies are lower, revealing potential challenges in knowledge transfer to the testing phase. In Fig. 6, the confusion matrix illustrates the model's performance in classifying fault conditions in solar PV modules: normal, breakage, cell damage, partial shading, and soiling. Notably, partial shading shows 437 correct classifications, with 2 misclassified as breakage, 1 as cell damage, 8 as normal, and 2 as soiling. Tab. 5 outlines the performance metrics, showing the proposed model outperforms pre-trained models, achieving a classification accuracy of 97,2%, as depicted in Fig. 7. Tab. 6 presents a detailed summary of the performance metrics for the PV fault detection model.

Table 3 Tuning parameters of Classifier

Optimizer	Learning rate	Number of epochs	Testing Accuracy / %	Training Accuracy / %
ADAM	0,01	5	85,72	86,52
		10	85,83	87,63
		15	84,12	85,02
	0,001	5	84,84	85,64
		10	86,28	88,08
		15	86,52	87,32
	0,0001	5	85,51	86,41
		10	86,23	88,13
		15	86,81	87,61
RMS prop	0,01	5	89,12	89,79
		10	89,49	90,29
		15	89,23	91,93
	0,001	5	89,47	91,27
		10	90,2	90,35
		15	89,94	90,74
	0,0001	5	90,18	91,08
		10	91,56	92,36
		15	91,54	91,34
StochasticGradient Descent (SGD)	0,01	5	92,67	92,68
		10	92,89	94,69
		15	94,12	95,02
	0,001	5	94,69	95,49
		10	97,20	97,52
		15	96,12	98,02
	0,0001	5	96,67	97,57
		10	95,67	97,47
		15	95,5	96,3

The model demonstrates exceptional precision (99,1%) and recall (97,2%) for the accurate classification of cell damage, leading to an overall accuracy of 97,24%. Both micro-average and macro-average classification scores consistently stand at 97,24% and 97,2%, respectively. Additionally, an ablation study was conducted to validate these classification results. This study involved removing specific layers, with corresponding details outlined in Tab. 5. Notably, the exclusion of MBConv layers in blocks 1, 4, and 5 affected both testing and training accuracy, reinforcing that the proposed PV fault classification model outperforms ablation experiments. The study highlights that removing layers negatively impacts model performance, further emphasizing its robustness. Extended experiments demonstrated that certain faults, such as partial shading and cell damage, were detected more accurately at non-perpendicular angles. For example, the 45° angle was most effective for detecting partial shading (92,4%) and breakage (89,7%), while the 90° (nadir) angle yielded the highest accuracy for normal conditions (90,8%) and soiling (86,2%). The 12 MP camera was particularly effective in enhancing fault detection for cell damage (85,7%), capturing finer details as shown in Tab. 7.

Table 4 Hyperparameter of the proposed network

Hyperparameter	Value
Validation Frequency	50
Initial Learning Rate	0,001
Epochs	5
Mini batch size	8
Gradient clipping	Gradient Threshold
Optimizer	Adam
Device type	GPU

These extended experiments revealed that both image resolution and shooting angles play critical roles in improving classification accuracy. Higher resolution images provided more detailed insights into subtle faults, such as micro-cracks. Moreover, non-perpendicular angles, particularly 45°, proved more effective in identifying specific issues such as partial shading and breakage. In contrast, for broader conditions like soiling and normal circumstances, the 90° angle was optimal, ensuring minimal distortion and achieving the highest accuracy for these types of faults. These findings underscore the importance of carefully selecting both camera specifications and shooting conditions to enhance the performance of fault detection models.

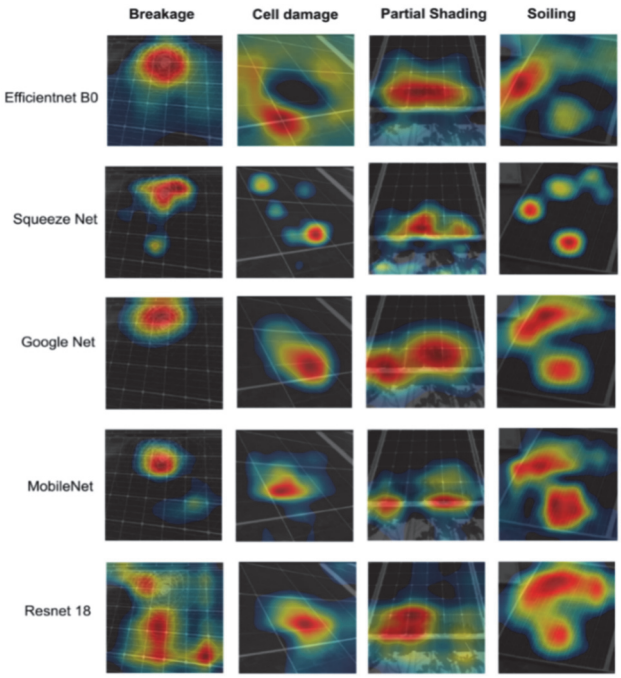

Figure 4 Class Activation Mapping Results: Squeezenet, Resnet 18, Googlenet, EfficientNet B0, and MobileNet V2

Table 5 Details of ablation study

Removed layer	Resolution	#Channels	#Layers	Training Accuracy / %	Testing Accuracy / %
Block 1-MB conv 1 K 3 × 3	112 × 112	32	1	78,25	75,38
Block 4-MB conv 6 K 3 × 3	28 × 28	40	1	82,16	80,20
Block 5 -MB conv 6 K 5 × 5	28 × 28	40	1	85,85	84,13
Block 5 -MB conv 6 K 5 × 5	28 × 28	40	1	86,26	83,34

Table 6 Efficientnet B0 classification performance

Metrics / Classes	Precision / %	Recall / %	F1 Score / %	Accuracy (Testing) / %
Normal	97,8	99,3	98,5	97,24
Breakage	94	99,3	96,6	
Partial Shading	98,2	93,2	95,6	
Soiling	97,1	97,5	97,2	
Cell damage	99,1	97,2	98,1	

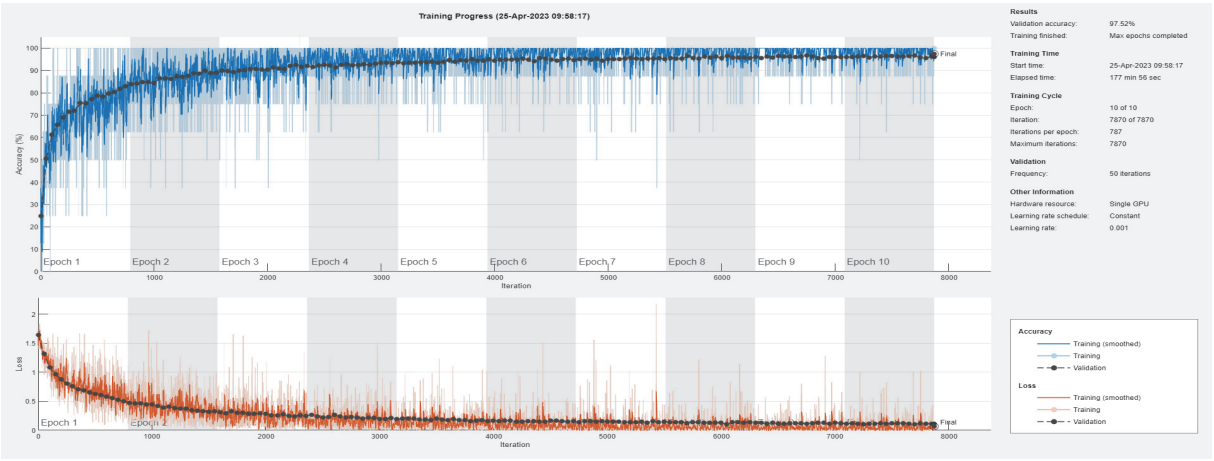

Figure 5 The Proposed Model's training plot

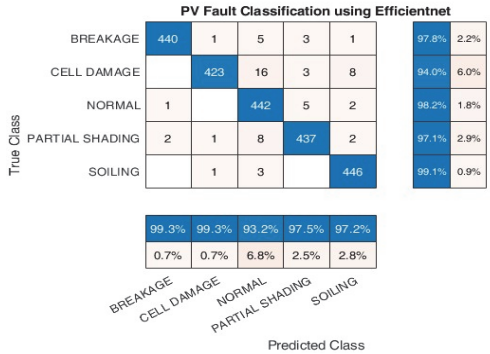

Figure 6 Confusion matrix for PV fault classification using EfficientNet B0

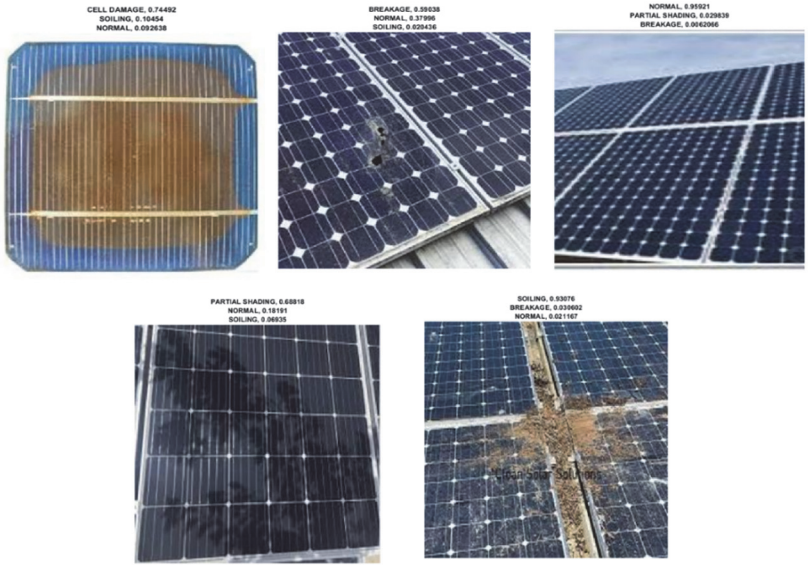

Figure 7 Testing results of PV fault classification

The efficiency of the proposed model has been evaluated using the ROC curve, which plots the True Positive Rate (TPR) against the False Positive Rate (FPR) at varying threshold values to distinguish normal from fault conditions. Fig. 8 displays the ROC for the local dataset, with the FPR on the horizontal axis and the TPR on the vertical axis. Different colored curves represent different fault classes. Notably, the green curve, positioned higher and separately from the others, corresponds to the breakage fault class. In Fig. 6 (failure case), normal conditions are misclassified as partial shading, and partial shading is misclassified as breakage, highlighting the higher accuracy for the breakage class compared to the others. The proposed EfficientNet B0 model outperforms traditional CNNs in PV panel fault classification due to its compound scaling, which optimizes network depth, width, and input resolution. This optimization enables efficient feature extraction and enhances computational performance. Unlike traditional approaches that rely on fixed-altitude, nadir-angle drone captures, manual image captures at 25° and 45° angles were employed, utilizing image transformation techniques to recreate a 90° angle. This method minimizes distortion and approximates the consistency of nadir captures, leading to improved fault detection accuracy. Furthermore, the model's capability to process high-resolution images allows it to detect fine defects, such as hairline cracks, resulting in an improved classification accuracy of 97,2%. Our diverse dataset, featuring various environmental conditions, further enhances the model's generalization to real-world scenarios. The empirical evaluation of the proposed classification model using existing pre-trained networks is presented in Tab. 8. Testing accuracy varies between 88% and 98%, depending on the model characteristics. Notably, the proposed model exhibits shorter computational and training times compared to other pre-trained models, except for Squeezenet, which is attributed to its reduced number of layers. Additionally, it achieves a significant accuracy improvement of 2,26% when compared with the ResNet 18 pre-trained model. It is important to highlight that the EfficientNet B0 model outperforms the other pre-trained CNNs. Fig. 7 presents sample test images from the PV fault condition system. A comparison of the proposed fault classification method with existing PV fault classification approaches is provided in Tab. 9. Approach [14] achieves an accuracy of 95,07% with a dataset of 3150 image samples, while algorithms like CNN [11] exhibit a lower accuracy of 73%. In contrast, the proposed method attains an accuracy of 97,2% when trained with a dataset comprising 11250 images. The performance evaluation of fault classification using EfficientNet B0 is compared to other CNN models, including VGG 19, CNN, Multiscale CNN, and ensemble models. Tab. 9 illustrates that EfficientNet B0 achieves higher accuracy. The proposed classification model is trained and tested on the benchmark data listed in Tab. 10. The aerial image dataset [7] and PV thermal image dataset [8], both of nearly equal sizes, show accuracies of 58,76% and 57,24%, respectively, due to the small dataset size. The infrared solar module dataset, comprising 20000 images, demonstrates an accuracy ranging from 77% to 83%, depending on the number of classes chosen for classification. Sample misclassified conditions are presented in Fig. 9, which represents the 2,8% inaccuracies of the EfficientNet B0 model.

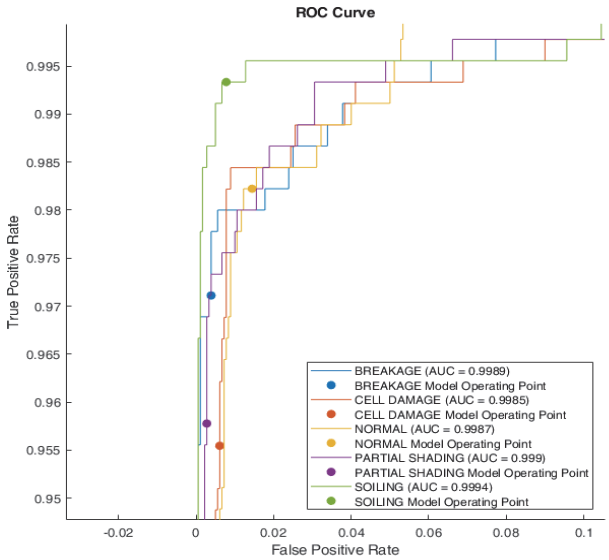

Figure 8 ROC of the trained Efficientnet B0 model

Table 7 Camera characteristics versus Accuracy

Camera Characteristics		Accuracy / %				
		Normal	Breakage	Partial Shading	Soiling	Cell damage
Resolution / Focal Length	3024 × 4032 / 26 mm	89,3	88,9	86,7	87,2	85,7
	1920 × 1080 /25 mm	87,7	86,3	85,4	86,1	80,7
Shooting angles	0°	85,6	88,1	83,2	90,1	84,8
	25°	86,4	87,8	84,5	87,4	89,3
	45°	87,9	89,7	92,4	86,1	88,7
	90	90,8	88,4	87,6	86,2	82,8

Table 8 Comparison of computational expenses of proposed model versus existing pre-trained model (train and test time in seconds)

Type of network	Training Accuracy / %	Computational time (Training)	Testing Accuracy / %	Computational time (Testing / Image)
Squeeze net	91,67	170 min 58 sec	88,04	60,10
Resnet 18	97,22	182 min 29 sec	94,98	106,95
Mobile net	97,07	242 min 7 sec	95,86	109,44
Google net	96,03	200 min 34 sec	94,49	157,80
Proposed model EfficientnetB0	97,52	177 min 56 sec	97,24	100,18

Table 9 Performance Comparison of existing Solar Fault Detection Methods Over the Standard and Proposed dataset

Reference	Dataset Name	Model	Accuracy / %	
			Dataset in literature	Local dataset
Sridharan et al. (2021)	Aerial images dataset	CNN	95,07	54,65
Raorane et al. (2022)	PV thermal images Dataset	VGG19	92	51
Le et al. (2021)	Infrared Solar Modules dataset	Ensemble model	86	90,77
Alves et al.(2021)	InfraredSolarModules dataset	CNN	78,85	55,65
Korkmaz et al. (2022)	Infrared Solar Modules dataset	Multi-Scale CNN	93,51	85,62
Duranay (2023)	Infrared Solar Modules dataset	Exemplar Efficientb0 model.	93,93	92,84
Proposed work	Compiled Dataset	Efficient net B0	-	97,2

Table 10 Comparative Performance Analysis of the Proposed Model against Existing Datasets

Paper	Dataset	Type of Image	Dataset Size	No. of class	Accuracy / %
Sridharan et al. (2021)	Aerial images dataset	RGB	3150	6	58,76
Raorane et al. (2022)	PV thermal Images Dataset	Thermographic	3336	3	57,24
Le et al. (2021)	Infrared Solar Modules (ISM) dataset	Infrared	20000	12	77,14
Korkmaz et al. (2022)	ISM dataset	Infrared	20000	11	79,12
Alves et al.(2021)	ISM dataset	Thermographic	20000	8	82,65
Duranay (2023)	ISM dataset	Infrared	20000	12	90,76
Proposed work	Compiled Dataset	RGB	11250	5	97,2

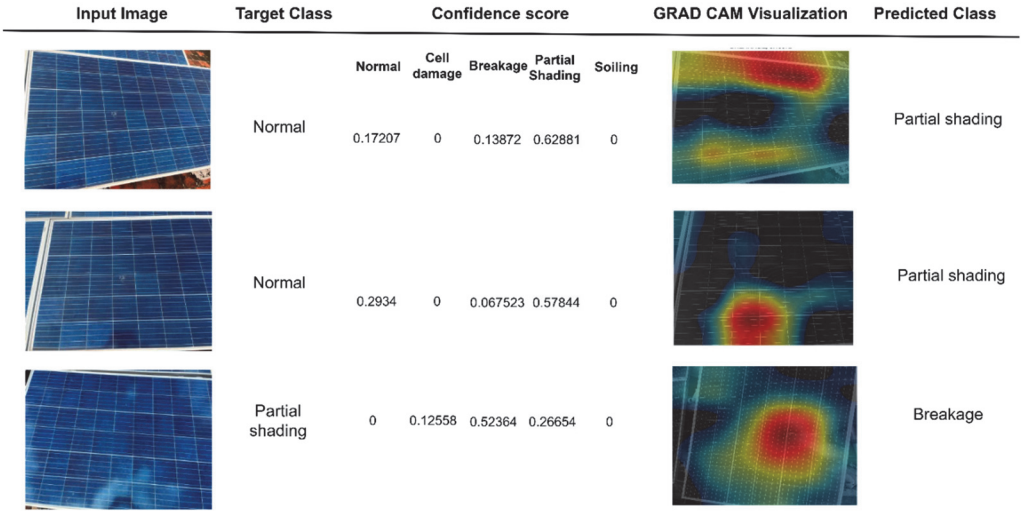

Figure 9 Misclassified Instances by the Trained Network

5 CONCLUSION

The proposed fault classification model for PV modules, based on the EfficientNet B0 architecture and a transfer learning approach, detects critical visual faults such as soiling, partial shading, cell damage, and glass breakage, which are essential for ensuring the operational efficiency and longevity of PV systems. The model achieves a high classification accuracy of 97,24%, providing a reliable solution for automating fault detection, reducing manual inspections, and lowering maintenance costs. By capturing RGB images under diverse environmental conditions and utilizing image augmentation techniques, the dataset reflects the variability encountered in real-world PV systems. This enhances the model's generalizability, allowing it to maintain high accuracy across various operational scenarios, which is crucial for minimizing missed detections and enabling faster interventions, thereby improving energy output and system performance. The model's scalability facilitates seamless integration into existing PV monitoring systems, supporting real-time fault detection in both small and large-scale solar installations. Comparative studies validate the model's superior performance over other pre-trained models and benchmark datasets, further reinforcing its industrial relevance. This approach offers a reliable, efficient, and adaptable solution to enhance PV system monitoring, reduce operational downtime, and contribute to the advancement of solar energy infrastructure.

Acknowledgement

The authors express their gratitude to the Thiagarajar College of Engineering (TCE) for supporting us to carry out this research work. Also, the financial support from TCE under Thiagarajar Research Fellowship scheme (File.no: TRF/Jul-2022/03) is gratefully acknowledged.

6 REFERENCES

[1] D'Adamo, I., Gastaldi, M., & Morone, P. (2020). The post-COVID-19 green recovery in practice: Assessing the profitability of a policy proposal on residential photovoltaic plants. *Energy Policy, 147*, 111910. https://doi.org/10.1016/j.enpol.2020.111910

[2] Perveen, G., Rizwan, M., Goel, N., & Anand, P. (2020). Artificial neural network models for global solar energy and photovoltaic power forecasting over India. *Energy Sources, Part A Recover. Util. Environ. Eff.*,1-26. https://doi.org/10.1080/15567036.2020.1826017

[3] Venkatesh, S. N., Jeyavadhanam, B. R., Sizkouhi, A. M., Esmailifar, S. M., Aghaei, M., & Sugumaran, V. (2022). Automatic detection of visual faults on photovoltaic modules

using deep ensemble learning network. *Energy Reports, 8*, 14382-14395. https://doi.org/10.1016/j.egyr.2022.10.427

[4] Arunachalam, V., Karthickraja, J., & Senthamizh Selvan, S. (2023). Wavelet transform-based detection, classification, and location of faults in a PV array. *Journal of Ambient Intelligence and Humanized Computing*, 1-11. https://doi.org/10.1007/s12652-023-04628-3

[5] Abubakar, A., Jibril, M. M., Almeida, C. F., Gemignani, M., Yahya, M. N., & Abba, S. I. (2023). A Novel Hybrid Optimization Approach for Fault Detection in Photovoltaic Arrays and Inverters Using AI and Statistical Learning Techniques: A Focus on Sustainable Environment. *Processes, 11*(9), 2549. https://doi.org/10.3390/pr11092549

[6] Badr, M. M., Hamad, M. S., Abdel-Khalik, A. S., Hamdy, R. A., Ahmed, S., & Hamdan, E. (2021). Fault Identification of Photovoltaic Array Based on Machine Learning Classifiers. *IEEE Access, 9*, 159113-159132. https://doi.org/10.1109/ACCESS.2021.3130889

[7] Garoudja, E., Chouder, A., Kara, K., & Silvestre, S. (2017). An enhanced machine learning-based approach for failure detection and diagnosis of PV systems. *Energy conversion and management, 151*, 496-513. https://doi.org/10.1016/j.enconman.2017.09.019

[8] Madeti, S. R. & Singh, S. N. (2018). Modeling of PV system based on experimental data for fault detection using the kNN method. *Solar Energy, 173*, 139-151. https://doi.org/10.1016/j.solener.2018.07.038

[9] Sun, J., Sun, F., Fan, J., & Liang, Y. (2017). Fault diagnosis model of photovoltaic array based on least squares support vector machine in Bayesian framework. *Applied Sciences, 7*(11), 1199. https://doi.org/10.3390/app7111199

[10] Basnet, B., Chun, H., & Bang, J. (2020). An intelligent fault detection model for fault detection in photovoltaic systems. *Journal of Sensors, 2020*(1). https://doi.org/10.1155/2020/6960328

[11] Venkatesh, S. N., Jeyavadhanam, B. R., Sizkouhi, A. M., Esmailifar, S. M., Aghaei, M., & Sugumaran, V. (2022). Automatic detection of visual faults on photovoltaic modules using deep ensemble learning network. *Energy Reports, 8*, 14382-14395. https://doi.org/10.1016/j.egyr.2022.10.427

[12] Niazi, K. A. K., Akhtar, W., Khan, H. A., Yang, Y., & Athar, S. (2019). Hotspot diagnosis for solar photovoltaic modules using a Naive Bayes classifier. *Solar Energy, 190*, 34-43. https://doi.org/10.1016/j.solener.2019.07.063

[13] Venkatesh, S. N. & Sugumaran, V. (2022). A combined approach of convolutional neural networks and machine learning for visual fault classification in photovoltaic modules. *Proceedings of the Institution of Mechanical Engineers, Part O: Journal of Risk and Reliability, 236*(1),148-159. https://doi.org/10.1177/1748006X211020305

[14] Sridharan, N. V. & Sugumaran, V. (2021). Convolutional neural network-based automatic detection of visible faults in a photovoltaic module. *Energy Sources, Part A: Recovery, Utilization, and Environmental Effects*, 1-16. https://doi.org/10.1080/15567036.2021.1905753

[15] Raorane, A., Magare, D., & Mistry, Y. (2022). Performance of fault classification on Photovoltaic modules using Thermographic images. *ITM Web of Conferences, 44*, 03065. https://doi.org/10.1051/itmconf/20224403065

[16] Álvarez-Tey, G. & García-López, C. (2022). Strategy Based on Two Stages for IR Thermographic Inspections of Photovoltaic Plants. *Applied Sciences, 12*(13), 6331. https://doi.org/10.3390/app12136331.

[17] Tao, X., Zhang, D., Ma, W., Liu, X., & Xu, D. (2018). Automatic metallic surface defect detection and recognition with convolutional neural networks. *Applied Sciences, 8*, 1-15. https://doi.org/10.3390/app8091575

[18] Akram, M. W., Li, G., Jin, Y., Chen, X., Zhu, C., Zhao, X., & Ahmad, A. (2019). CNN-based automatic detection of photovoltaic cell defects in electroluminescence images. *Energy, 189*, 116319. https://doi.org/10.1016/j.energy.2019.116319

[19] Li, X., Yang, Q., Lou, Z., & Yan, W. (2019). Deep Learning Based Module Defect Analysis for Large-Scale Photovoltaic Farms. *IEEE Trans. Energy Convers, 34*, 520-529. https://doi.org/10.1109/TEC.2018.2873358

[20] Duranay, Z. B. (2023). Fault Detection in Solar Energy Systems: A Deep Learning Approach. *Electronics, 12*(21), 4397. https://doi.org/10.3390/electronics12214397

[21] Cavieres, R., Barraza, R., Estay, D., Bilbao, J., & Valdivia-Lefort, P. (2022). Automatic soiling and partial shading assessment on PV modules through RGB images analysis. *Applied Energy, 306*, 1179640. https://doi.org/10.1016/j.apenergy.2021.117964

[22] Alves, R. H. F., de Deus Junior, G. A., Marra, E. G., & Lemos, R. P. (2021). Automatic fault classification in photovoltaic modules using Convolutional Neural Networks. *Renewable Energy, 179*, 502-516. https://doi.org/10.1016/j.renene.2021.07.070

[23] Korkmaz, D. & Acikgoz, H. (2022). An efficient fault classification method in solar photovoltaic modules using transfer learning and multi-scale convolutional neural network. *Engineering Applications of Artificial Intelligence, 113*, 104959. https://doi.org/10.1016/j.engappai.2022.104959

Contact information:

R. PRIYADARSHINI, Research Scholar
(Corresponding author)
Thiagarajar College Of Engineering,
Madurai 625 015 Tamilnadu, India
E-mail: priyaravikumar2015be@gmail.com

P. S. MANOHARAN, Professor
Thiagarajar College Of Engineering,
Madurai 625 015 Tamilnadu, India
E-mail: psmeee@tce.edu

S. MOHAMED MANSOOR ROOMI, Professor
Thiagarajar College Of Engineering,
Madurai 625 015 Tamilnadu, India
E-mail: smmroomi@tce.edu